Intraspecific variation of phragmocone chamber volumes throughout ontogeny in modern *Nautilus* and the Jurassic ammonite *Normannites*

Amane Tajika, Naoki Morimoto, Ryoji Wani, Carole Naglik, Christian Klug

Nautilus, the iconic living fossil, still has been of great interest for palaeontologists over a long period of time for actualistic comparisons and to speculate on aspects of the palaeoecology of fossil cephalopods, which are impossible to assess otherwise. Although a large amount of work has been dedicated to *Nautilus* ecology, their conch geometry and volumes have been studied only poorly. In addition, although the focus on volumetric analyses for ammonites has been increasing recently with the development of computed tomographic technology, the intraspecific variation of volumetric parameters has never been examined. To investigate the intraspecific variation of the phragmocone chamber volumes throughout ontogeny, 30 specimens of Recent *Nautilus pompilius* and two Middle Jurassic ammonites (*Normannites mitis*) were reconstructed using computed tomography and grinding tomography, respectively. Both of the ontogenetic growth trajectories from the two *Normannites* demonstrate logistic increase. However, a quite high difference in *Normannites* has been observed between their entire phragmocone volumes (cumulative chamber volumes), in spite of their similar morphology and size. Ontogenetic growth trajectories from *Nautilus* also show a high variation. Sexual dimorphism appears to contribute significantly to this variation. Finally, covariation between chamber widths and volumes was examined. The results illustrate the strategic difference in chamber construction between *Nautilus* and *Normannites*. The former genus persists to construct a certain conch shape, whereas the conch of the latter genus can change its shape flexibly under some constraints.

Intraspecific variation of phragmocone chamber volumes throughout ontogeny in modern *Nautilus* and the Jurassic ammonite *Normannites*

Amane Tajika[1], Naoki Morimoto[2] , Ryoji Wani[3], Carole, Naglik[1] and Christian Klug[1]

[1]Paläontologisches Institut und Museum, Universität Zürich, Karl Schmid-Strasse 4, CH-8006 Zürich, Switzerland

[2]Laboratory of Physical Anthropology, Graduate School of Science, Kyoto University, Kitashirakawa Oiwake-cho, Sakyo-ku 606-8502 Kyoto, Japan

[3]Faculty of Environment and Information Sciences, Yokohama National University, Yokohama, 240-8501, Japan

ABSTRACT

Nautilus, the iconic living fossil, remains of great interest to palaeontologists after a long history of actualistic comparisons and speculation on aspects of the palaeoecology of fossil cephalopods, which are otherwise impossible to assess. Although a large amount of work has been dedicated to *Nautilus* ecology, their conch geometry and volumes have been studied less frequently. In addition, although the focus on volumetric analyses for ammonites has been increasing recently with the development of computed tomographic technology, the intraspecific variation of volumetric parameters has never been examined. To investigate the intraspecific variation of the phragmocone chamber volumes throughout ontogeny, 30 specimens of Recent *Nautilus pompilius* and two Middle Jurassic ammonites (*Normannites mitis*) were reconstructed using computed tomography and grinding tomography, respectively. Both of the ontogenetic growth trajectories from the two *Normannites* demonstrate logistic increase. However, a quite high difference in *Normannites* has been observed between their entire phragmocone volumes (cumulative chamber volumes), in spite of their similar morphology and size. Ontogenetic growth trajectories from *Nautilus* also show a high variation. Sexual dimorphism appears to contribute significantly to this variation. Finally, covariation between chamber widths and volumes was examined. The results illustrate the strategic difference in chamber construction between *Nautilus* and *Normannites*. The former genus persists to construct a certain conch shape, whereas the conch of the latter genus can change its shape flexibly under some constraints.

Subjects Palaeontology, Zoology, Development

Keywords Ammonoidea, Nautilida, growth, 3D reconstruction, intraspecific variability, sexual dimorphism

INTRODUCTION

Ammonoids and nautiloids are well-known, long-lived molluscan groups, both of which faced devastation at the end of Cretaceous, but with different responses: extinction versus survival. What these two groups have in common is the external conch, which makes them superficially comparable. Because of that, a number of palaeontologists investigated the ecology and anatomy of living *Nautilus* as an analogy for those of extinct ammonites over the last decades (e.g., *Collins et al., 1980; Saunders & Landman, 1987; Ward, 1987; 1988*). However, it was *Jacobs & Landman (1993)* who argued that, despite its superficial morphologic similarity, *Nautilus* was an insufficient model to reconstruct ammonoid palaeoecology, given their phylogenetic positions, which are distant within the Cephalopoda. This argument is now widely accepted. While palaeoecology and evolution of ammonoids need to be discussed based on their own fossil record (or soft tissue preservation), those of modern *Nautilus* can be satisfactorily analogized to fossil nautilids, which have borne persistent conch morphologies throughout their evolution (*Ward, 1980*).

Molluscan conchs are not only exoskeletal structures but also records of their growth throughout the entire ontogeny because of their accretionary growth mechanism. One of the most important apomorphic structures of cephalopods, the chambered part of their conch (phragmocone), was and is used by most cephalopods as a buoyancy device. The ammonite phragmocone has been of great interest for palaeontologists, in order to reveal otherwise-obscure aspects of ammonite palaeoecology (Geochemical analyses: *Moriya et al., 2003*; *Lukeneder et al., 2010*; 2 dimensional analyses of septal angles: *Arai & Wani, 2012*). Until recently, buoyancy had not been examined by quantifying phragmocone volumes due to the lack of adequate methods. Now complete ammonite empirical volume models have been reconstructed expressly to calculate ammonoid buoyancy (*Lemanis et al., 2015; Naglik et al., 2015a; Tajika et al., 2015*). Unfortunately, all of these contributions included only one specimen per species due to the great expenditure of time needed for segmenting the image stacks. Conclusions from such limited studies may be biased if the examined specimens represent more or less extreme variants of one species (intraspecific variation). The lifemode of living *Nautilus* is known to be essentially demersal, retaining their buoyancy as either roughly neutral when active or slightly negative when at rest (*Ward & Martin, 1978*), even though they change their habitat frequently via vertical migration (*Dunstan et al., 2011*). The majority of *Nautilus* ecology research has included study of anatomy, behaviour, and habitat, whereas geometry and volume of their phragmocone, which are similar to that of fossil nautiloids, has scarcely been examined. Investigation of the relationship between *Nautilus* conchs and their ecology could become a reference to examine the relationship between fossil cephalopods and their palaeoecology.

Multiple methods have been applied to reconstruct conchs of cephalopods including both fossilized and extant animals (*Kruta et al., 2011; Naglik et al., 2015b;Hoffmann et al., 2014; Lemanis et al., 2015; Tajika et al., 2015*; for general aspects of virtual palaeontology, see *Garwood et al., 2010* and *Sutton et al., 2014*). Non-destructive computed tomography (CT) superficially appears to be the best suitable method because rare fossils can be analysed without destroying them. Medical scanners are often used, but they often yield insufficient contrast between conch and internal sediment or cement because these materials may have similar densities (e.g., *Kruta et al., 2011*). Furthermore, the resolution obtained from medical scanners is not adequate, specifically in such cases where accurate measurements of minute structures such as ammonite protoconchs (as small as 0.5 mm in diameter; e.g., *Lemanis et al., 2015*) are required. Fossil cephalopods are thus difficult materials to examine by this non-destructive method, but conchs of living cephalopods with no sediment filling can easily be reconstructed with a good resolution. Computed microtomography (µCT) is an alternative because it has a stronger beam, resulting in high resolution and thus better reconstructions. Even µCT-imagery produced using high energy levels can suffer from the lack of contrast, however, making the subsequent segmentation difficult.

By contrast, *Lemanis et al. (2015)* presented the first successful attempt to reconstruct an ammonite protoconch in detail. They scanned a perfectly preserved hollow ammonite using phase contrast tomography. Propagation phase contrast X-ray synchrotron microtomography (PPC-SR-µCT) was employed by *Kruta et al. (2011)* who reconstructed ammonite radulae in detail. The limited availability of the facility, heavy data load, and, new potential contrast problems discourage application this method for recent *Nautilus*. In contrast to the non-destructive methods, destructive grinding tomography can be used to reconstruct fossilized cephalopods (*Naglik et al., 2015b; Tajika et al., 2015*). This method, which gives sufficient contrast for segmentation, does not require hollow preservation of fossils, thus permitting the examination of all well-preserved fossils without suffering from noise such as beam hardening, partial volume effect, or poor contrast, which commonly occur when using CT. Abbreviation of the great expenditure of time needed to generate tomographic data is required to encourage wider use of this method.

Volumetric analyses of intraspecific variability of phragmocone chambers throughout ontogeny has not previously been analysed in either *Nautilus* or ammonoids. Such data may contribute to the better understanding of the palaeoecology of extinct ammonoids and nautiloids. The aims of this study are to answer the following questions based on empirical 3D models reconstructed from real specimens: (1) How did chamber volumes change through the development of ammonites and nautilids? (2) How much did the volumetric growth trajectories differ between two conspecific ammonites (exemplified using middle Jurassic *Normannites*)? (3) What was the intraspecific variation of volumetric growth trajectories of modern *Nautilus*? (4) Are the differences in chamber volumes between male and female nautilids significant? (5) Is there a difference in construction of chambers between the ammonites and modern *Nautilus*?

MATERIAL

Two ammonite specimens examined are from the Middle Jurassic and belong to the genus *Normannites*. One of them (Nm. 1) was reconstructed by *Tajika et al. (2015)* to test its buoyancy. Both specimens were found in the Middle Bajocian (Middle Jurassic) of Thürnen, Switzerland. The nicely preserved specimens are suitable for 3D reconstruction, even though one of the specimens (Nm. 2) has an incomplete aperture, which does not allow for buoyancy calculation. The maximum conch diameters of specimen1 and specimen 2 are 50.0 mm and 49.0 mm, respectively.

An additional 30 conchs of Recent *Nautilus pompilius* (21 adults: 12 males, 9 females; 9 juveniles) were also studied. All of the conchs were collected in the Tagnan area in the Philippines (see fig. 1 in *Wani, 2004*; fig. 1 in *Yomogida & Wani, 2013*). The details of the specimens are summarized in Table 1. The specimens are stored in Mikasa City Museum, Hokkaido, Japan.

METHODS

3D reconstructions of ammonites

Grinding tomography was employed to reconstruct the two Jurassic ammonite specimens. This method has been applied to previous studies for invertebrates, e.g., bivalves (*Götz, 2003; 2007; Götz and Stinnesbeck, 2003; Hennhöfer et al., 2012, Pascual-Cebrian et al., 2013*) and ammonoids (*Naglik et al., 2015b: Tajika et al., 2015*). During each of the numerous grinding phases, 0.06 mm was automatically ground off of the specimens until the specimen was completely destroyed. Subsequently, each ground surface was automatically scanned. Due to the very high number of slices and the very time consuming segmenting process, only every fourth scan of the obtained image stack were segmented. We separately segmented the external conch, all septa, and the siphuncle manually using Adobe® Illustrator. The segmented image stacks have been exported to VGstudiomax®2.1, which produced 3D models out of the 2D image stacks. Further technical details for the ammonite reconstructions are given in *Tajika et al. (2015)* and for the general procedure of grinding tomography in *Pascual-Cebrian et al. (2013)*.

3D reconstructions of modern *Nautilus*

Conchs of all specimens were scanned at the Laboratory of Physical Anthropology of Kyoto University using a 16-detector-array CT device (Toshiba Alexion TSX-032A) with the following data acquisition and image reconstruction parameters: beam collimation: 1.0 mm; pitch: 0.688; image reconstruction kernel: sharp (FC30); slice increment: 0.2 mm. This resulted in volume data sets with isotropic spatial resolution in the range of 0.311 and 0.440 mm. The obtained data sets were exported to Avizo®8.1 where segmentation was conducted. As mentioned in *Hoffmann et al. (2014)*, the calculated mass of a specimen based on the CT data set does not correspond exactly to the actual mass measured on the physical specimen due to noise from the scan, which may cause significant errors during the segmentation process. In our scans, the resulting differences between the actual masses of the conchs and the calculated mass ranged from 50 to 63%. However, as the noise which affects segmentation occurs uniformly over the entire scan when the same devices and methods are used a combination of the same grey-scale threshold value for the outer whorls and the manual tracing for the innermost whorls preserves the variability in volumes between each specimen. Out of 45 scanned specimens, only 30 scanned specimens with nearly the same contrast were carefully chosen and analysed, while scans from other 15 specimens with different contrasts were discarded to minimize errors which may occur from differences in contrast between scans. The segmented data sets were exported as STL files using the software Avizo®8.1 and were then processed in Meshlab and Matlab 8.5 (Math Works) to extract the volumetric data from the phragmocone. The measurements of the diameters and widths of the conchs were conducted with the program ForMATit developed by NM.

RESULTS

Difference between two *Normannites* specimens in ontogenetic volume changes

Constructed 3D models of the ammonites are shown in Fig. 1. Measured chamber volumes (Table 2) were plotted against chamber numbers (Fig. 2). In the two *Normannites*, the overall trends of growth trajectories of individual chamber volumes (Fig. 2A) are more or less the same, showing logistic increase throughout ontogeny until the onset of the so-called '*morphologic countdown*' (*Seilacher and Gunji, 1993*) when they start showing a downward trend over the last 5 chambers (Nm. 1) and over the last 7 chambers (Nm. 2). The curve from Nm. 1 illustrates a nearly steady growth rate even though a *syn vivo* epizoan worm with mineralized tube grew on the fifth whorl of the ammonite *(Tajika et al., 2015)*. By contrast, Nm. 2 does not show traces of any *syn vivo* epizoan, but it displays a sudden decrease of the volume of the 45th chamber where another trend sets off, which persists to the last chamber. In addition, we plotted the cumulative volumes of the phragmocone chambers against chamber numbers (Fig. 2B). Since the curves are derivatives of those of Fig. 2, the phragmocone volumes increase with the same trend. The cumulative phragmocone volume of Nm. 1 is larger than that of Nm. 2, although the latter retained the larger phragmocone volume throughout ontogeny until the onset of the morphologic countdown.

Intraspecific variability of modern *Nautilus* in ontogenetic volume changes

Constructed 3D models of modern *Nautilus* are shown in Fig. 3. As in the Jurassic ammonite, individual chamber volumes and phragmocone volumes (Table 3) were plotted against chamber numbers (Fig. 3A; B). Fig. 3 shows that all the curves increase logistically, as in the ammonites, with quite high variability. As far as the morphologic countdown is concerned, only the last or no chamber of adult specimens shows the volume decrease. By contrast, the two ammonites show this decrease over the last 5 to 7 chambers (even higher numbers of chambers may be included in other ammonite species: e.g., 18 in the Late Devonian *Pernoceras*, 14 in the Early Carboniferous *Ouaoufilalites*; see *Korn et al., 2010; Klug et al., 2015*) bearing the irregular growth. In order to assess the differences between male and female conchs, their growth trajectories are shown in Fig. 4. Maximum diameters of the conchs versus number of chambers (Fig. 5A) and maximum diameters versus phragmocone volumes are also plotted (Fig. 5B) to assess if previously-recognized morphologic differences between males and females of *Nautilus* are detectable here.

Comparison of chamber formation between ammonites and *Nautilus*

Widths (for *Normannites*: Table 2; for *Nautilus*: Table 4) and volumes of each chamber were plotted against chamber numbers for the ammonites (Fig. 6) and *Nautilus* (Fig. 7). It should be noted that the widths of each chamber for the ammonites may not be very accurate. For instance, for the widths of the 42nd to 44th chamber of Nm. 2 (Fig. 6B), we obtained the same value (7.7 mm), which presumably does not represent the actual width. This has been caused by the reduction in resolution resulting from segmenting only every 4th slice with an increment between two images 0.24 mm in voxel z (instead of 0.06 mm; see the method chapter above for details). In addition to the low resolution, the obscure limit between chambers and septa at the edges of the chambers (on the flanks) in the slices might also have resulted in some errors in segmentation. However, the overall trend of the widths through ontogeny should still be correctly depicted and thus the errors mentioned above were negligible for our (Fig. 6B).

DISCUSSION

Ontogenetic volumetric growth of ammonites

Due to preservation and limited resolution, the chambers in the first two whorls of the Jurassic ammonites could not be precisely measured. There appears to be a subtle point where the slope of the curves changes at around the 28 to 29th chamber (Fig. 2B), corresponding to a conch diameter of about 4.5 mm. This change may represent the end of the second growth stage of ammonoids, the neanic stage, because it has been reported that the neanic stage of ammonoids lasts until a conch diameter of 3-5 mm *(Bucher et al., 1996)*. This point may have been related to the change of their mode of life, i.e. from planktonic to nektoplanktonic or nektonic *(Arai and Wani, 2012)*. Taking this into account, the first two whorls of the conch comprise the first two growth stages, namely the embryonic and the neanic stages (*Bucher et al., 1996; Westermann, 1996; Klug, 2001*). Note that since the volumes of chambers formed earlier than 25th and 27th in Nm. 1 and Nm. 2 have not been measured due to the poor resolution, the transition between the first two growth stages has not been examined. The last several chamber numbers display fluctuating growth known as morphological countdown (*Seilacher and Gunji, 1993*). In Nm. 2, an abrupt decrease of chamber volume occurred at the 45th chamber, marking another trend resulting in a lower cumulative volume than in Nm. 1. It is known that injuries affect the septal spacing in modern *Nautilus* as well as in ammonoids (*Kraft et al., 2008*). However, there are no visible injuries on the conch of Nm. 2, suggesting that this might have not been the case. Although the ammonite could have repaired a shell injury, it would be hard to recognize the presence of such a sublethal injury due to low resolution or the effects of shell replacement. Environmental changes might also have affected the conch construction. For example, in modern scleractinian corals, it is suggested that the Mg/Ca ratio in the sea water alters the conch growth rate (*Ries et al., 2006*). The knowledge of the sedimentary facies of the host rock from which the ammonites were extracted is insufficient to identify possible causes for the alteration of shell growth. Another possibility is the presence of parasites such as tube worms. They might have grown on the external conch, which affected the buoyancy of the ammonite. Because of the absence of any trace of *syn vivo* epifauna on the conch, this scenario is unlikely. Interestingly, Nm. 1 preserves the trace of a worm tube in the fifth whorl (*Tajika et al., 2015*), which had no detectable effect on chamber formation (Fig. 2A).

The two different cumulative volumes of phragmocone chambers should result in a difference in buoyancy, given that the size of the two ammonites is more or less equal. The buoyancy of Nm. 1 was calculated by *Tajika et al. (2015)* as being positively buoyant in the (unlikely) absence of cameral liquid. Based on these calculations, they estimated the fill fraction of cameral liquid to attain neutral buoyancy as being about 27 %. Unfortunately, the incompleteness of the aperture of Nm. 2 does not permit us to calculate the buoyancy. It is quite reasonable, however, to speculate that Nm. 2 requires slightly more cameral liquid to reach neutral buoyancy (>27 %) because of its size, its smaller phragmocone, and the probably nearly identical conch mass. The fact that morphologically-similar specimens of the same species (*Normannites mitis*) likely expressed variation in buoyancy raises the question whether morphologically diverse genera like *Amaltheus* (*Hammer & Bucher, 2006*) also varied in buoyancy regulation.

Ontogenetic volumetric growth of modern *Nautilus* and its intraspecific variation

Landman et al. (1983) reported that the first seven septa of Recent *Nautilus* are more widely spaced than the following ones; the point where septal spacing changes lies between the 7th and 8th chamber. It is considered to correspond to the time of hatching, which is also reflected in the formation of a shell-thickening and growth halt known as nepionic constriction. This feature is also reported from fossil nautilids (*Landman et al., 1983; Wani & Ayyasami, 2009, Wani & Mapes, 2010*). Our results reveal a constant growth rate until the 5th or 6th chamber (Fig. 4B). Thereafter, the growth changes to another constant growth rate. Differences in the position of the nepionic constriction may be an artifact of low resolution of the scan, which might have made the very first (and possibly the second) chamber invisible. Nevertheless, in each examined specimen the chamber volumes fluctuate but typically increase until the appearance of the nepionic constriction (Table 3). At the mature growth stage, most specimens show a volume reduction of the last chamber. Variability in chamber volume could be a consequence of several factors that influence the rate of chamber formation (growth rate): temperature, pH (carbon saturation degree), trace elements, food availability, sexual dimorphism, injuries, and genetic predisposition for certain metabolic features.

A relevant model for shell growth may be the 'temperature size rule' (e.g., *Atkinson, 1994*) which states that the growth rate slows down and the body size increases under extremely high or low temperatures. If this rule is applicable to the examined *Nautilus*, the temperature might have changed the growth rate of each individual because vertical migration of *Nautilus* is reported to range from near the sea surface to about 700 m (*Dunstan et al., 2011*). *Dunstan et al. (2011)* also suggested that the strategy for vertical migration of geographically separated *Nautilus* populations may vary depending on the slope, terrain and biological community. At this point, it is hard to conclude whether or not the temperature size rule applies because the behaviour of *Nautilus* in the Philippines can be highly different from Australian *Nautilus* as reported by *Dunstan et al., 2011*. According to *Ward & Chamberlain (1983)*, the period of chamber formation of *Nautilus pompilius* ranges from 85 to 132 days. It is still likely that one individual inhabited different water columns from other individuals, producing varying trends of growth trajectories. Tracking the behaviour of modern *Nautilus* in the Philippines may provide more information on the role and applicability of the temperature size rule.

Analyses of stable isotopes have been used to estimate habitats of shelled animals (e.g., *Landman et al., 1994; Moriya et al. 2003; Auclair et al., 2004*; *Lécuyer & Bucher, 2006; Lukeneder et al., 2010; Ohno et al., 2014*). It might be worthwhile to examine the isotopic composition of the shells of a few nautilid and ammonoid shells with different volumetric change through ontogeny, because this may yield some information on the relationships between habitat and growth trajectories.

The pH (or carbon saturation degree) is important for shell secretion. This means that the decrease of carbon saturation causes a lack of CO_3^{2-}-ions, which are required to produce aragonitic or calcitic shells (e.g., *Ries et al., 2009*). This change in pH may alter the time needed to form a chamber and thereby reduce or increase the chamber volume. Similarly, trace elements like the Mg/Ca ratio in the sea water can affect the growth rate (for corals see, e.g., *Ries et al., 2006*). Food availability is also a possible explanation for the great variation. *Strömgren & Cary (1984)* demonstrated a positive correlation between growth rate of mussels and food source. It is likely that there was at least some competition for food between *Nautilus* individuals and probably also with other animals. The individuals in a weaker position might have had access to less food or food of poorer quality.

Intraspecific variability can also originate from sexual dimorphism. In the case of *Nautilus*, males tend to be slightly larger than females with slightly broader adult body chambers (*Hayasaka et al., 2010; Saunders &Ward, 2010; Tanabe & Tsukahara 2010*). However, in the juvenile stage, the morphological differences are not very pronounced, thus often making sexing difficult. The two slopes in the curves of chamber volumes obtained from males and females were compared using a test (analysis of the residual sum of squares) described in *Zar (1984)*. This test was conducted independently for the embryonic stage and the other growth stages since the critical point between the 5th and the 6th chamber changes the slope of the growth curve (Fig. 4B). Moreover, an analysis of the residual sum of squares for nonlinear regressions was performed to compare the two logistic models of males and females for the latter stage (Fig. 4C). No significant difference in the embryonic stage and a significant difference in the later stage (Table 5 and 6) suggest that the differentiation in chamber volume between both sexes begins immediately after hatching. The results (Fig. 4) also show, however, the occurrence of conch morphologies common to both sexes. Taking this into account, their volume is not an ideal tool for sexing. The same statistical test for linear regressions was also conducted to compare the number of formed chambers (Fig. 5A) and the phragmocone volume (Fig. 5B) with maximum conch diameter between male and female individuals. The test results (Table 5) appear to imply that there is a significant difference between the female and male in both cases, although the significance levels are not strict (the number of chambers vs. maximum diameter: $P<0.05$: the entire phragmocone volume vs. maximum diameter: $P<0.1$). A greater sample, however, may yield a clearer separation. The results of a series of statistical tests (Table 5; analyses of the residual sum of squares) suggest that the males tend to produce more chambers, potentially indicating a prolonged life span or less energetic investment in reproduction. The addition of another chamber to males could be associated with their sexual maturity; the weight of the large spadix and a large mass of spermatophores in males might necessitate more space and buoyancy. *Ward et al. (1977)* reported that the total weight of males of *Nautilus pompilius* from Fiji exceeds that of females by as much as 20 %. What remains unclear is the reason why females tend to have larger phragmocone volumes than males while they are immature. It is true, however, that even within each sex, the variability of the total phragmocone volumes is quite high (standard deviation for males: 15.4; for females: 13.4; for both males and females: 14.3)

Injuries are visible in several of the examined specimens, yet there is no link to a temporal or spatial change in chamber volume in the growth curves. *Yomogida & Wani (2013)* examined injuries of *Nautilus pompilius* from the same locality in the Philippines, reporting traces of frequent sublethal attacks rather early in ontogeny than in later stages. The frequency of sublethal attacks early in ontogeny may be one of the factors determining the steepness of the grow trajectory curves. This aspect can be tested in further studies. Additionally, morphological variability may also root in genetic variability but the causal link is difficult to test.

Covariation of chamber volumes and widths in ammonoids and nautiloids

The relationship between chamber volumes of *Nautilus pompilius* (Fig. 7) revealed that their chamber widths expanded at a constant pace irrespective of the change in chamber volume. *Nautilus* may be designed to maintain a rather constant conch morphology with the buoyancy regulation depending largely on septal spacing only. By contrast, the chamber widths and volumes of the ammonites appear to covary (Fig. 6). This distinct covariation may have partially contributed to the high morphological variability with some constraints in response to fluctuating environmental conditions or predatory attacks (for details, see the discussion for *Nautilus* above). This aspect, however, needs to be examined further using an image stack of an ammonite with a higher resolution and better preservation to rule out artefacts.

CONCLUSIONS

We virtually reconstructed the conchs of two Middle Jurassic ammonites (*Normannites mitis*) and 30 specimens of Recent nautilids (*Nautilus pompilius*) using grinding tomography and computed tomography (CT), respectively, to analyse the intraspecific variability in volumetric change of their chambers throughout ontogeny. The data obtained from the constructed 3D models led to the following conclusions:

1. Chamber volumes of *Normannites mitis* and *Nautilus pompilius* were measured to compare the ontogenetic change. The growth trajectories from the two *Normannites mitis* and *Nautilus pompilius* follow logistic curves throughout most of their ontogeny. The last several chambers of the two *Normanites mitis* show fluctuating chamber volumes, while most specimens of *Nautilus pompilius* demonstrate volume reduction of only the last chamber.
2. Growth trajectories of the two *Normannites mitis* specimens were compared. The two specimens appear to have a transition point between the 28th and 29th chamber from which the slopes of their growth curves change, which has been documented in previous. However, their entire phragmocone volumes differ markedly despite the two shells sharing similar morphology and size. Intraspecific variation of buoyancy was not testable in this study due to the low sample number. This aspect needs to be addressed in future research because buoyancy analyses could provide information on the habitat of ammonoids.
3. Growth trajectories of thirty *Nautilus pompilius* conchs show a high variability.
4. Results of statistical tests for *Nautilus pomplilius* corroborate that the variability is increased by the morphological difference between the two sexes: adult males are larger than females. This may be ascribed to the formation of voluminous sexual organs in the male. Individual chamber volumes of the female tend to be larger than those of males. The results also show that intraspecific variability within one sex is reasonably strong.

Examinations of their injuries, isotopic analyses of the examined conchs or tracking the behaviour of *Nautilus* could yield more information on the relationship between their variability in chamber volumes and ecology. Such data could help to reconstruct the palaeoecology of fossil nautiloids and possibly also of extinct ammonoids.

5. Covariation between the chamber widths and volumes in ammonites and *Nautilus pompilius* were examined. The results illustrate that conch construction of *Nautilus pompilius* is robust, maintaining a certain shape, whereas the conchs of the examined ammonite were more plastic, changing their shapes during growth under some fabricational constraints. Further investigations need to be carried out to verify the covariation between widths and volumes of ammonites with other variables such as conch thickness, conch width, and perhaps buoyancy using a reconstruction method with a higher resolution and perfectly-preserved materials.

ACKNOWLEDGEMENT

We would like to thank Dominik Hennhöfer and Enric Pascual Cebrian (Universität Heidelberg) for carrying out the grinding tomography. Beat Imhof (Trimbach) kindly donated the two specimens of *Normannites*. We are also thankful to Torsten Scheyer (Universität Zürich) for the introduction to the use of Avizo® 8.1. Kathleen Ritterbush (University of Chicago) proofread the manuscript and corrected the English. A fruitful discussion with Kozue Nishida (The Geological Survey of Japan) is greatly appreciated.

ADDITIONAL INFORMATION AND DECLARATIONS

Funding

This study is supported by the Swiss National Science Foundation SNF (project numbers 200020_132870, 200020_149120, and 200021_149119).

Author Contributions.

- Amane Tajika conceived, designed the study, wrote most of the manuscript, prepared the figures and tables, reviewed drafts of the paper.
- Naoki Morimoto contributed his experience in CT-scanning and segmenting, reviewed drafts of the paper. He also put his software [illegible]isposal.
- Ryoji Wani collected conchs of *Nautilus pompilius*, reviewed drafts of the paper.
- Carole Naglik contributed her experience in grinding tomography and handling of image stacks, reviewed drafts of the paper.
- Christian Klug wrote parts of the text, contributed ideas for some measurements and tests, edited the manuscript, reviewed drafts of the paper.

REFERENCES

Arai K, Wani R. 2012. Variable growth modes in late cretaceous ammonoids: implications for diverse early life histories. *Journal of Paleontology* **86**:258–267.

Atkinson D. 1994. Temperature and organism size—a biological law for ectotherms? *Advances in Ecological Research* **25**:1–58.

Auclair AC, Lécuyer C, Bucher H, Sheppard SMF. 2004. Carbon and oxygen isotope composition of *Nautilus macromphalus*: a record of thermocline waters off New Caledonia. *Chemical Geology* **207**:91–100.

Bucher H, Landman NH, Klofak SM, Guex J. 1996. Mode and rate of growth in ammonoids. In Landman NH, Tanabe K, Davis RA, eds. *Ammonoid paleobiology*. New York, Plenum, 407–461.

Collins D, Ward PD, Westermann GEG. 1980. Function of cameral water in *Nautilus*. *Paleobiology* **6**:168–172.

Dunstan AJ, Ward PD, Marshall NJ. 2011. Vertical distribution and migration patterns of *Nautilus pompilius*. *PloS one* **6(2)**:e16311.

Garwood RJ, Rahman IA, Sutton MD. 2010. From clergymen to computers – the advent of virtual palaeontology. *Geol Today* **26(3)**:96–100.

Götz S. 2003. Larval settlement and ontogenetic development of Hippuritella vasseuri (DOUVILLE´) (Hippuritoidea, Bivalvia). *GeolCroat* **56(2)**:123–131.

Götz S. 2007. Inside rudist ecosystems: growth, reproduction and population dynamics. In: Scott RW, editor. Cretaceous rudists and carbonate platforms: environmental feedback. SEPM Special Publication Vol. 87. Tulsa (OK): *Society for Sedimentary Geology* 97–113.

Götz S, Stinnesbeck W. 2003. Reproductive cycles, larval mortality and population dynamics of a Late Cretaceous hippuritid association: a new approach to the biology of rudists based on quantitative threedimensional analysis. *Terra Nova* **15(6)**:392–397.

Hammer Ø, Bucher H. 2006. Generalized ammonoid hydrostatics modelling, with application to *Intornites* and intraspecific variation in *Amaltheus*. *Palaeontological Research* **10**:91–96.

Hayasaka S, Ōki K, Tanabe K, Saisho T, Shinomiya A. 2010. On the habitat of *Nautilus pompilius* in Tanon Strait (Philippines) and the Fiji Islands. In Saunders WB, Landman NH, eds. *Nautilus. The Biology and Paleobiology of a living fossil.* Springer: Dordrecht, 179–200.

Hennhöfer, DK, Götz S, Mitchell SF .2012. Palaeobiology of a Biradiolites mooretownensis rudist lithosome: seasonality, reproductive cyclicity and population dynamics. *Lethaia* **45(3)**, 450-461.

Hoffmann R, Schultz JA, Schellhorn R, Rybacki E, Keupp H, Gerden SR, Lemanis R, Zachow S. 2014. Non-invasive imaging methods applied to neo- and paleontological cephalopod research. *Biogeosciences Discussions* **10**:18803–18851.

Jacobs DK, Landman NH. 1993. Nautilus—a poor model for the function and behavior of ammonoids?. *Lethaia* **26(2):**101–111.

Klug C. 2001. Life-cycles of Emsian and Eifelian ammonoids (Devonian). *Lethaia* **34**:215–233.

Klug C, Zatoń M, Parent H, Hostettler B, Tajika A. 2015. Mature modifications and sexual dimorphism. In Klug C, Korn D, De Baets K, Kruta I, Mapes RH, eds. *Ammonoid paleobiology, Volume I: from anatomy to ecology*. *Topics in Geobiology* **43**, Springer: Dordrecht, 70 pp.

Korn D, Bockwinkel J, Ebbighausen V. 2010. The ammonoids from the Argiles de Teguentour of Oued Temertasset (early Late Tournaisian; Mouydir, Algeria). *Fossil Record* **13**:35–152.

Kraft S, Korn D, Klug C. 2008. Ontogenetic patterns of septal spacing in Carboniferous ammonoids. *Neues Jahrbuch für Geologie und Mineralogie, Abh* **250**:31–44.

Kruta I, Landman N, Rouget I, Cecca F, Tafforeau P. 2011. The role of ammonites in the Mesozoic marine food web revealed by jaw preservation. *Science* **331(6013)**:70-72.

Landman NH, Rye DM, Shelton KL. 1983. Early ontogeny of *Eutrephoceras* compared to Recent Nautilus and Mesozoic ammonites: evidence from shell morphology and light stable isotopes. *Paleobiology* **9**:269–279.

Landman NH, Cochran JK, Rye DM, Tanabe K, Arnold JM. 1994. Early Life History of *Nautilus*: Evidence from Isotopic Analyses of Aquarium-Reared Specimens. *Paleobiology* **20**:40-51.

Lemanis R, Zachow S, Fusseis F, Hoffmann R. 2015. A new approach using high-resolution computed tomography to test the buoyant properties of chambered cephalopod shells. *Paleobiology* **41(02)**:313-329.

Lécuyer C, Bucher H. 2006. Stable isotope compositions of a late Jurassic ammonite shell: a record of seasonal surface water temperatures in the southern hemisphere? *eEarth Discuss* **1**:1-19.

Lukeneder A, Harzhauser M, Müllegger S, Piller, WE. 2010. Ontogeny and habitat change in Mesozoic cephalopods revealed by stable isotopes ($\delta^{18}O$, $\delta^{13}C$). *Earth and Planetary Science Letters* **296**:103–114.

Moriya K, Nishi H, Kawahata H, Tanabe K, Takayanagi Y. 2003. Demersal habitat of Late Cretaceous ammonoids: Evidence from oxygen isotopes for the Campanian (Late Cretaceous) northwestern Pacific thermal structure. *Geology* **31**:167–170.

Naglik C, Rikhtegar F, Klug C. 2015a. Buoyancy of some Palaeozoic ammonoids and their hydrostatic properties based on empirical 3D-models. *Lethaia*. DOI: 10.1111/let.12125

Naglik C, Monnet C, Götz S, Kolb C, De Baets K, Tajika A, Klug C. 2015b. Growth trajectories of some major ammonoid sub‐clades revealed by serial grinding tomography data. *Lethaia* **48(1)**:29-46.

Ohno A, Miyaji T, Wani R. 2014. Inconsistent oxygen isotopic values between on temporary secreted septa and outer shell walls in modern Nautilus. *Lethaia*. DOI:10.1111/let.12109.

Pascual-Cebrian E, Hennhöfer DK, Götz S. 2013. 3D morphometry of polyconitid rudist bivalves based on grinding tomography. *Facies* **59(2)**:347-358.

Ries JB, Stanley SM, Hardie LA. 2006. Scleractinian corals produce calcite, and grow more slowly, in artificial Cretaceous seawater. *Geology* **34**:525–528.

Ries JB, Cohen AL, McCorkle DC. 2009. Marine calcifiers exhibit mixed responses to CO2-induced ocean acidification. *Geology* **37(12)**:1131-1134.

Saunders WB, Ward PD. 2010. Ecology, distribution, and population characteristics of *Nautilus*. In Saunders WB, Landman NH, eds. *Nautilus. The Biology and Paleobiology of a living fossil.* Springer: Dordrecht, 137–162.

Saunders WB, Landman, NH. (eds.). 1987. *Nautilus: The Biology and Paleobiology of a Living Fossil.* New York: Plenum.

Seilacher A, Gunji YP. 1993. Morphogenetic countdown: another view on heteromorph shells in gastropods and ammonites. *Neues Jahrb Geol Paläontol* **190**:237–265.

Strömgren T, Cary C. 1984. Growth in length of *Mytilus edulis* L. fed on different algal diets. *Journal of experimental marine biology and ecology* **76**:23–34.

Sutton M, Rahman I, Garwood R. 2014. *Techniques for Virtual Palaeontology*. Chichester: Wiley-Blackwell.

Tajika A, Naglik C, Morimoto N, Pascual-Cebrian E, Hennhöfer D, Klug C. 2015. Empirical 3D model of the conch of the Middle Jurassic ammonite microconch *Normannites*: its buoyancy, the physical effects of its mature modifications and speculations on their function. *Historical Biology* **27(2)**:181-191.

Tanabe K, Tsukahara J. 2010. Biometrie analysis of *Nautilus pompilius* from the Philippines and the Fiji Islands. In Saunders WB, Landmann NH, eds. *Nautilus: The Biology and Paleobiology of a Living Fossil.* Springer Netherlands.

Wani R. 2004. Experimental fragmentation patterns of modern *Nautilus* shells and the implications for fossil cephalopod taphonomy. *Lethaia* **37**:113–123.

Wani R, Ayyasami K. 2009. Ontogenetic change and intra-specific variation of shell morphology in the Cretaceous nautiloid (Cephalopoda, Mollusca) Eutrephoceras clementinum (d'Orbigny, 1840) from the Ariyalur area, southern India. Journal of *Paleontology* **83(3)**:365–378.

Wani R, Mapes RH. 2010. Conservative evolution in nautiloid shell morphology; evidence from the Pennsylvanian nautiloid Metacoceras mcchesneyi from Ohio, USA. Journal of *Paleontology* **84(3)**:477-492.

Ward PD. 1980. Comparative shell shape distributions in Jurassic-Cretaceous ammonites and Jurassic-Tertiary nautilids. *Paleobiology* **6**:32–43.

Ward PD. 1987. The natural history of *Nautilus*, 1-267.

Ward PD. 1988. *In search of Nautilus.* New York: Simon & Schuster.

Ward PD, Chamberlain J. 1983. Radiographic observation of chamber formation in *Nautilus pompilius*. *Nature* **304:**57–59.

Ward P, Stone R, Westermann G, Martin A. 1977. Notes on animal weight, cameral fluids, swimming speed, and colour polymorphism of the cephalopod *Nautilus pompilius* in the Fiji Islands. P*aleobiology* **3(4)**:377–388.

Westermann GEG. 1996. Ammonoid life and habitat. In Landman NH, Tanabe K, Davis RA, eds. *Ammonoid paleobiology*. New York, Plenum, 607–707.

Yomogida S, Wani R. 2013. Higher risk of fatality by predatory attacks in earlier ontogenetic stages of modern *Nautilus pompilius* in the Philippines: evidence from the ontogenetic analyses of shell repairs. *Lethaia* **46**:317–330.

CAPTIONS

Figure 1 3D reconstructions of the two specimens of *Normannites mitis*, modern *Nautilus pompilius* (specimen 17), and their phragmocones. (1A) 3D model of *Normannites mitis* (Nm. 1); (1B) 3D model of *Normannites mitis* (Nm. 2); (1C) extracted phragmocone of Nm. 1 (1C); extracted phragmocone of Nm. 2; (2A, B) 3D models of *Nautilus pompilius* (specimen 17); (2C) extracted phragmocone of *Nautilus pompilius* (specimen 17); (2D) Backface of 3D model of *Nautilus pompilius* (specimen 17). Scale bars are 1 cm.

Figure 2 Volumes plotted against chamber numbers in *Normannites mitis*. The volumes prior to chamber 25 (Nm. 1) and 27 (Nm. 2) have not been measured. (A) Scatter plot of chamber numbers and individual chamber volumes. (B) Scatter plot of chamber numbers and cumulative phragmocone volumes.

Figure 3 Chamber volumes plotted against chamber numbers in all examined *Nautilus pompilius*. (A) scatter plot of chamber numbers and individual chamber volumes . (B) scatter plot of chamber numbers and phragmocone volumes.

Figure 4 Comparison between males and females. Chamber volumes plotted against chamber numbers in *Nautilus pompilius*. Squares and diamonds represent the female and male, respectively. (A) scatter plot of chamber numbers and individual volumes; (B) semilog scatter plot of chamber numbers and individual volumes. (C) scatter plot of chamber numbers and cumulative phragmocone volumes.

Figure 5 Comparison between males and females. Squares, diamonds, and triangles represent the female, male, and indeterminable sex, respectively. (A) scatter plot of maximum conch diameters and chamber numbers of a specimen; (B) scatter plot of maximum conch diameters and the phragmocone volume.

Figure 6 Volumes and widths of chambers plotted against chamber numbers in *Normannites mitis*. Squares and diamonds represent volumes and widths, respectively. (A) Nm.1; (B) Nm. 2.

Figure 7 Volumes and widths of chambers plotted against chamber numbers in *Nautilus pompilius*. Squres and diamonds represent volumes and widths, respectively. (A) Specimen 8; (B) Specimen 7; (C) specimen 53. Specimens with different growth trajectories were analysed.

Table 1 Details of the studied specimens, *Normannites mitis* from the Middle Jurassic, Switzerland, and modern *Nautilus pompilius* from the Philippines.

Table 2 Raw data of measured chamber volumes and widths in *Normannites mitis*.

Table 3 Raw data of measured chamber volumes in *Natutilus pompilius*.

Table 4 Raw data of measured chamber widths of *Natutilus pompilius*.

Table 5 Results of statistical tests (analyses of the residual sum of squares) comparing linear regressions of males and female. N, number of samples; RSS; residual sum of squares; DF, degree of freedom; ns, not significant; s; significant.

Table 6 Results of a statistical test (an analysis of the residual sum of squares) comparing nonlinear regressions of males and females. RSS; residual sum of squares; DF, degree of freedom; ns, not significant; s; significant.

Figure 1 (on next page)

3D reconstructions of the two specimens of *Normannites mitis*, modern *Nautilus pompilius* (specimen 17), and their phragmocones.

(1A) 3D model of *Normannites mitis* (Nm. 1); (1B) 3D model of *Normannites mitis* (Nm. 2); (1C) extracted phragmocone of Nm. 1 (1C); extracted phragmocone of Nm. 2; (2A, B) 3D models of *Nautilus pompilius* (specimen 17); (2C) extracted phragmocone of *Nautilus pompilius* (specimen 17); (2D) Backface of 3D model of *Nautilus pompilius* (specimen 17). Scale bars are 1 cm.

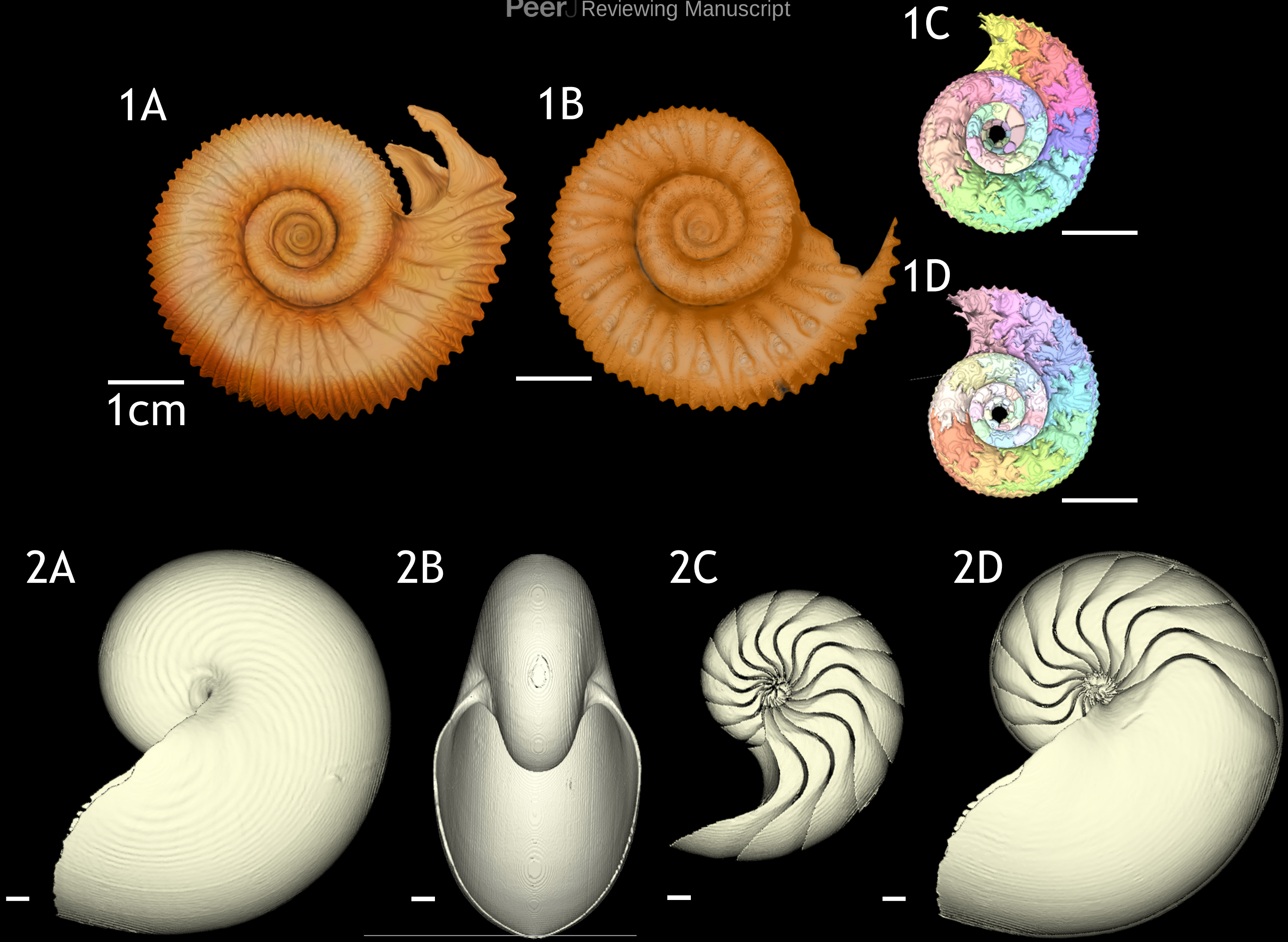
1A
1B
1C
1D
1cm
2A
2B
2C
2D

Figure 2 (on next page)

Volumes plotted against chamber numbers in *Normannites mitis*. The volumes prior to chamber 25 (Nm. 1) and 27 (Nm. 2) have not been measured.

(A) Scatter plot of chamber numbers and individual chamber volumes. (B) Scatter plot of chamber numbers and cumulative phragmocone volumes.

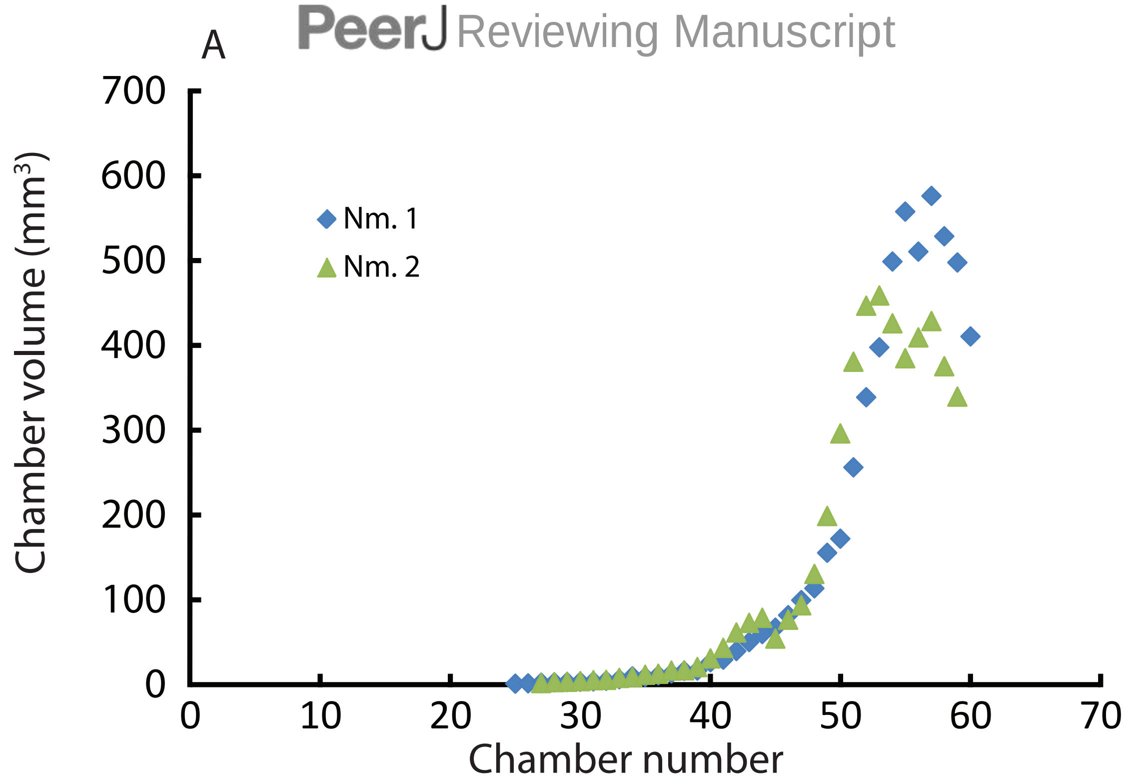
A
Chamber volume (mm³)
700
600
500
400
300
200
100
0
Nm. 1
Nm. 2
0
10
20
30
40
50
60
70
Chamber number

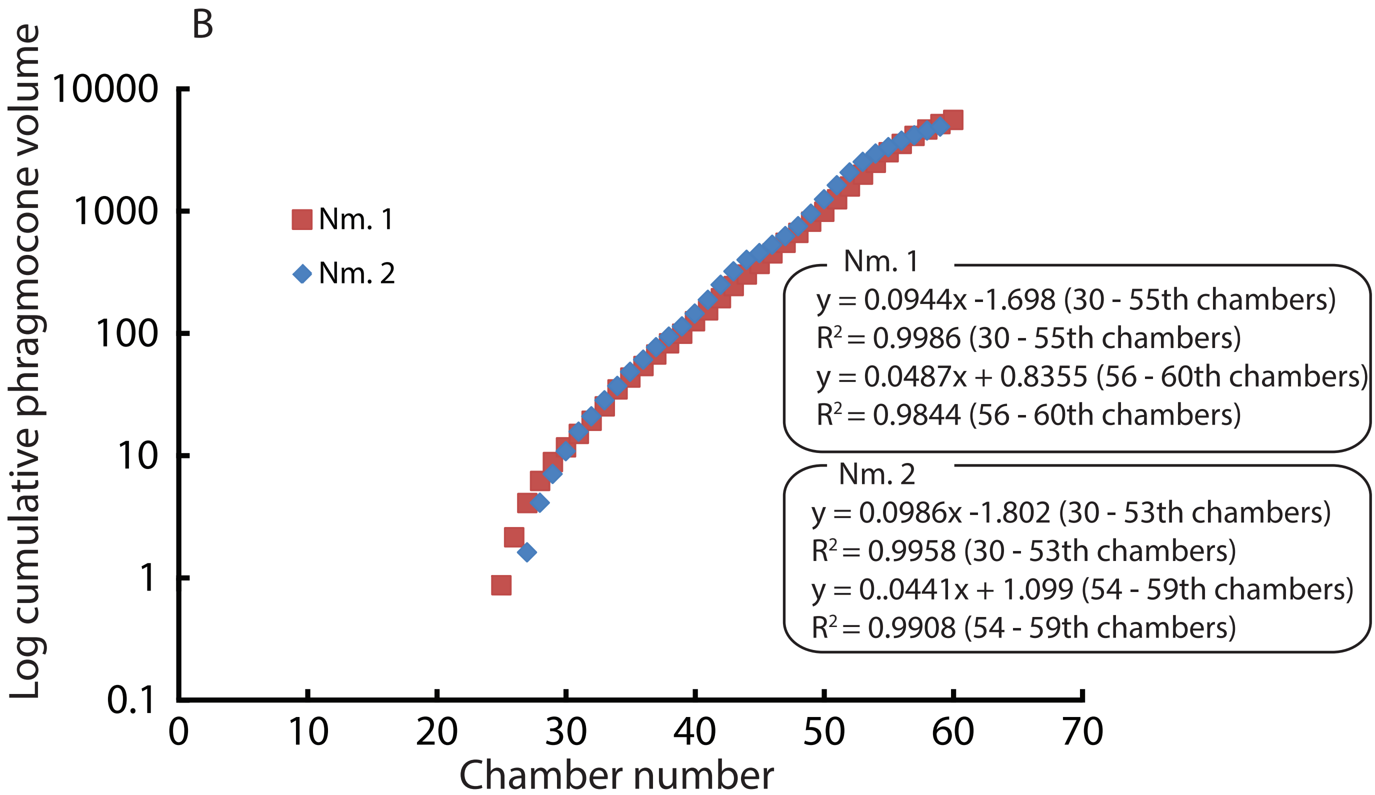
B
Log cumulative phragmocone volume
10000
1000
100
10
1
0.1
Nm. 1
Nm. 2
0
10
20
30
40
50
60
70
Chamber number
Nm. 1
y = 0.0944x -1.698 (30 - 55th chambers)
R² = 0.9986 (30 - 55th chambers)
y = 0.0487x + 0.8355 (56 - 60th chambers)
R² = 0.9844 (56 - 60th chambers)
Nm. 2
y = 0.0986x -1.802 (30 - 53th chambers)
R² = 0.9958 (30 - 53th chambers)
y = 0..0441x + 1.099 (54 - 59th chambers)
R² = 0.9908 (54 - 59th chambers)

Figure 3 (on next page)

Chamber volumes plotted against chamber numbers in all examined *Nautilus pompilius*.

(A) scatter plot of chamber numbers and individual chamber volumes . (B) scatter plot of chamber numbers and phragmocone volumes.

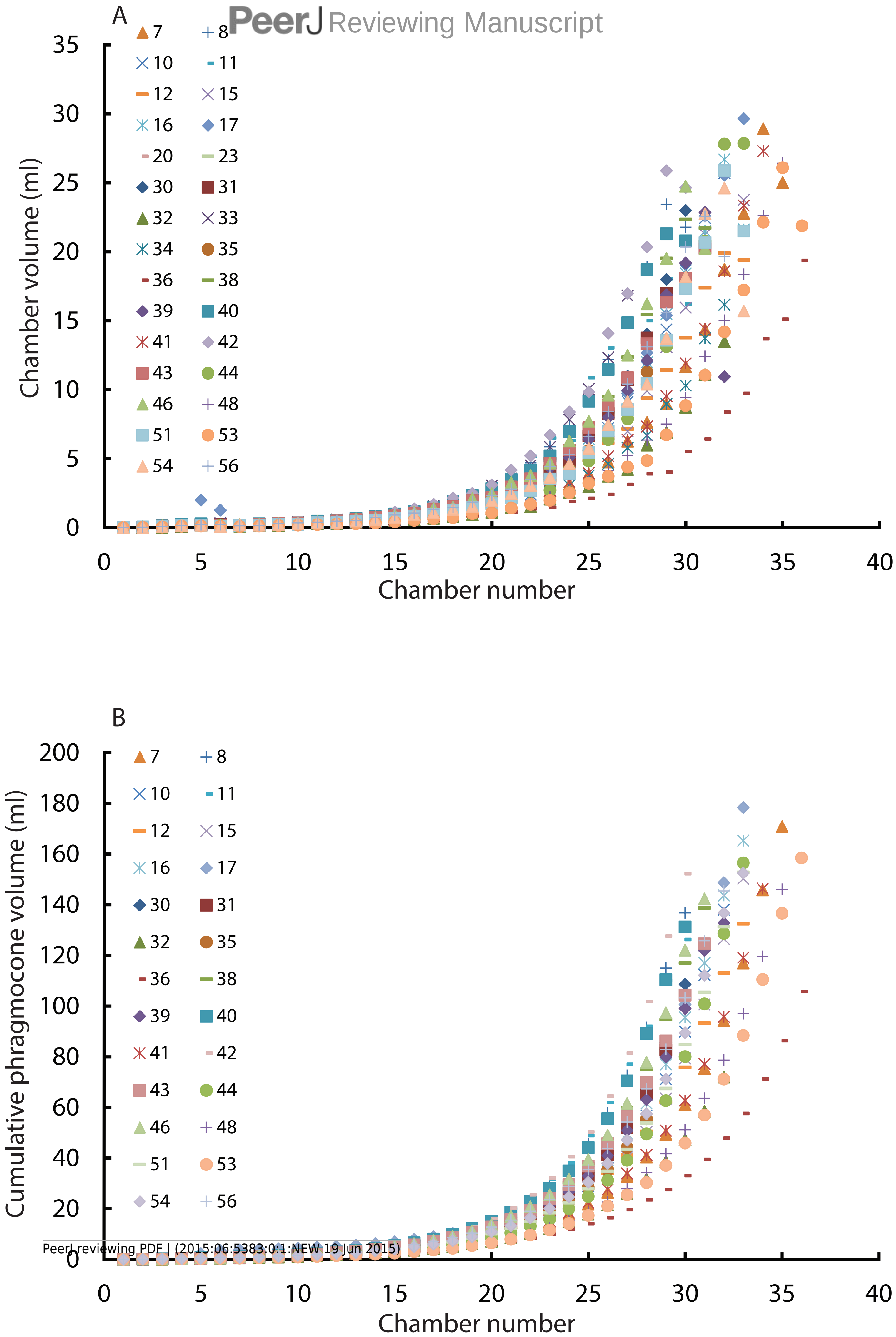
A
Chamber volume (ml)
Chamber number
7
8
10
11
12
15
16
17
20
23
30
31
32
33
34
35
36
38
39
40
41
42
43
44
46
48
51
53
54
56
B
Cumulative phragmocone volume (ml)
Chamber number
7
8
10
11
12
15
16
17
30
31
32
35
36
38
39
40
41
42
43
44
46
48
51
53
54
56

Figure 4(on next page)

Comparison between males and females. Chamber volumes plotted against chamber numbers in *Nautilus pompilius*. Squares and diamonds represent the female and male, respectively.

(A) scatter plot of chamber numbers and individual volumes; (B) semilog scatter plot of chamber numbers and individual volumes. (C) scatter plot of chamber numbers and cumulative phragmocone volumes.

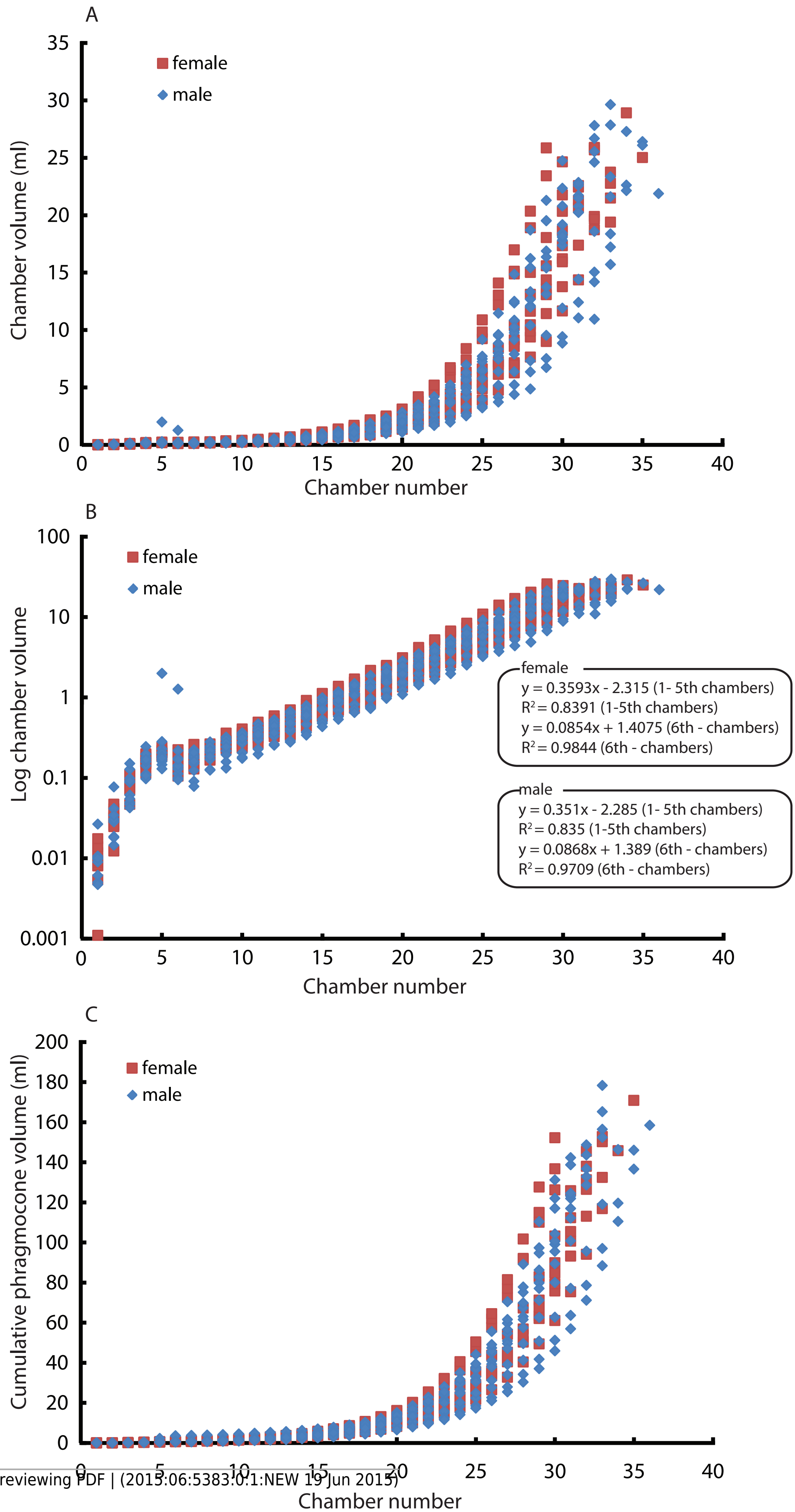

A
Chamber volume (ml)
Chamber number
female
male
B
Log chamber volume
Chamber number
female
male
female
y = 0.3593x - 2.315 (1- 5th chambers)
R² = 0.8391 (1-5th chambers)
y = 0.0854x + 1.4075 (6th - chambers)
R² = 0.9844 (6th - chambers)
male
y = 0.351x - 2.285 (1- 5th chambers)
R² = 0.835 (1-5th chambers)
y = 0.0868x + 1.389 (6th - chambers)
R² = 0.9709 (6th - chambers)
C
Cumulative phragmocone volume (ml)
Chamber number
female
male

Figure 5(on next page)

Comparison between males and females. Squares, diamonds, and triangles represent the female, male, and indeterminable sex, respectively.

(A) scatter plot of maximum conch diameters and chamber numbers of a specimen; (B) scatter plot of maximum conch diameters and the phragmocone volume.

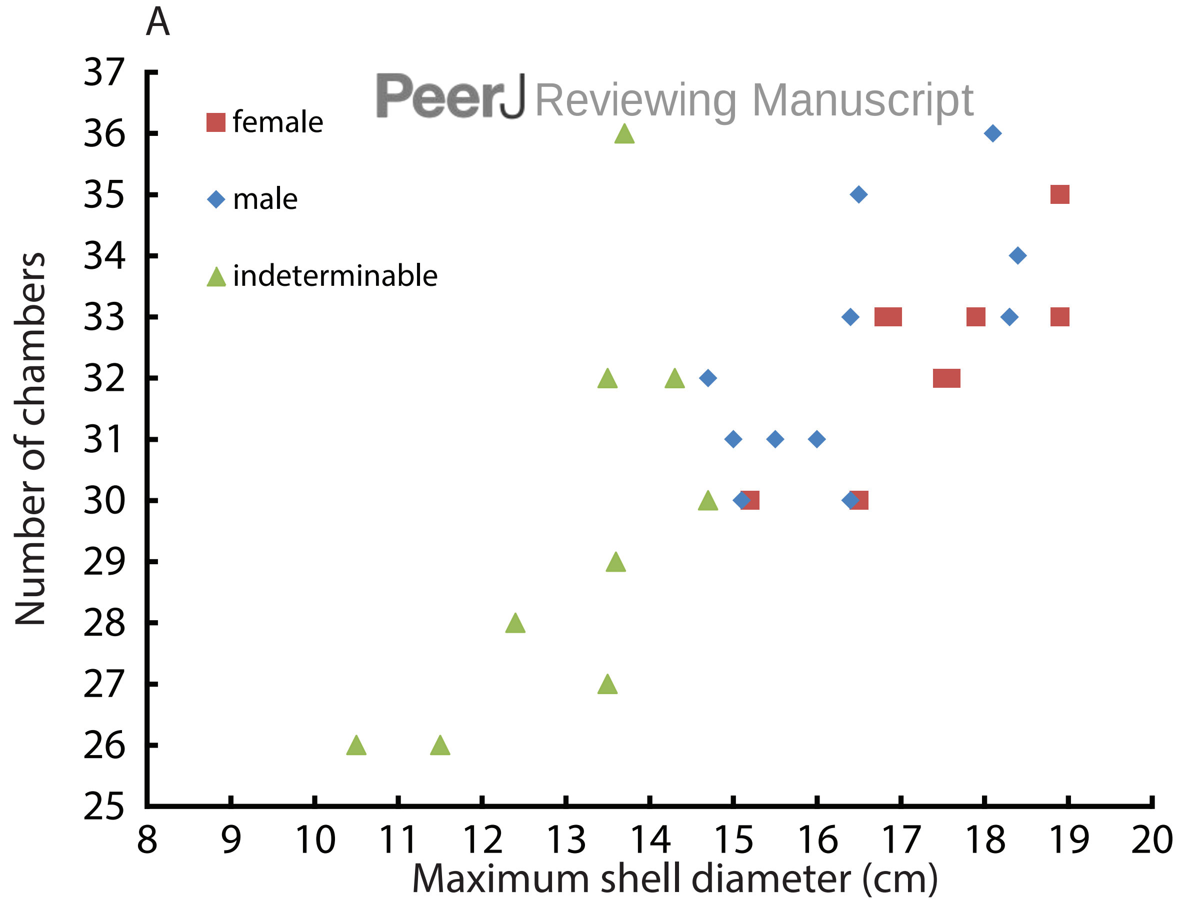
A
female
male
indeterminable
Number of chambers
37
36
35
34
33
32
31
30
29
28
27
26
25
8
9
10
11
12
13
14
15
16
17
18
19
20
Maximum shell diameter (cm)

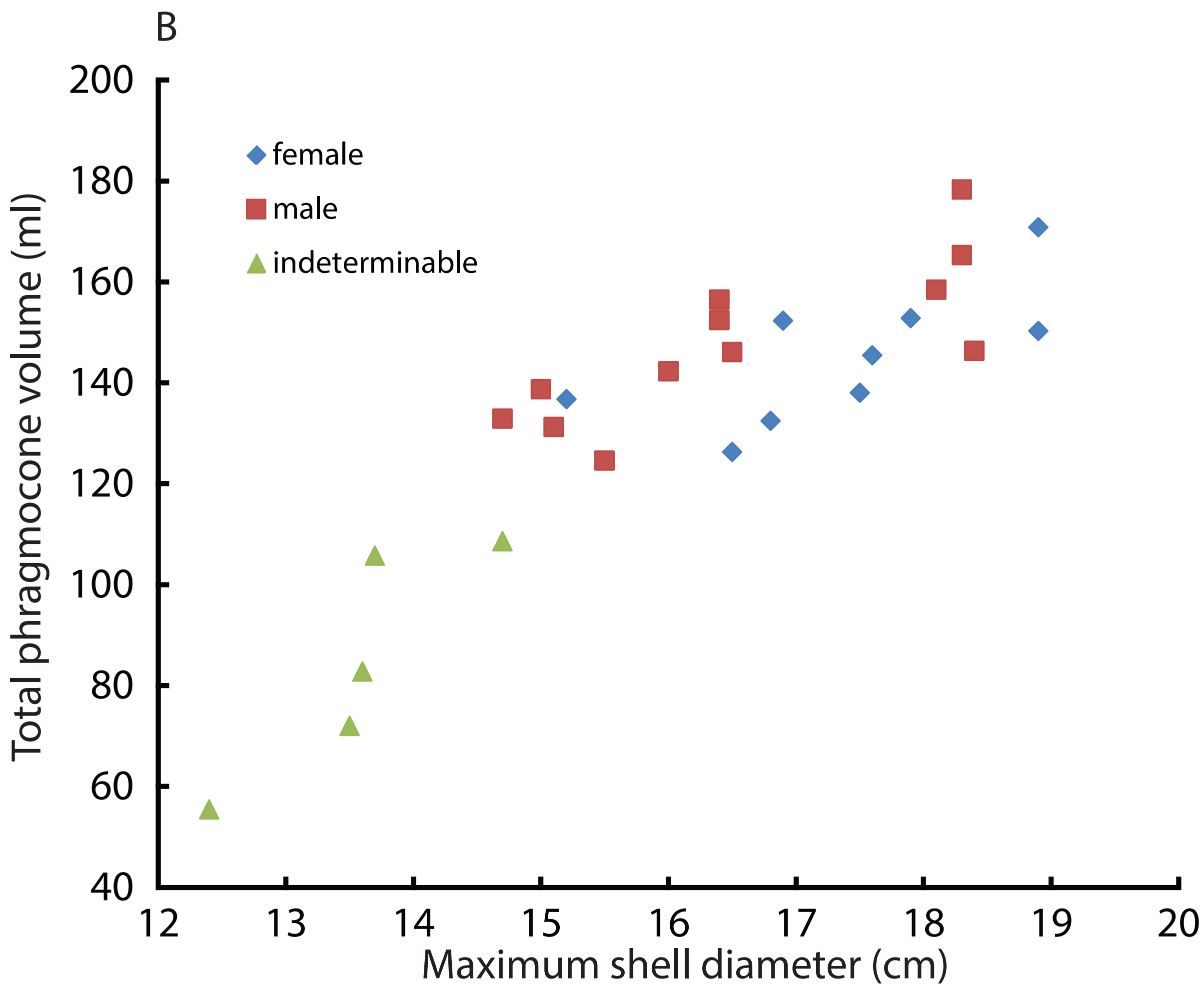
B
female
male
indeterminable
Total phragmocone volume (ml)
200
180
160
140
120
100
80
60
40
12
13
14
15
16
17
18
19
20
Maximum shell diameter (cm)

Figure 6 (on next page)

Volumes and widths of chambers plotted against chamber numbers in *Normannites mitis*. Squares and diamonds represent volumes and widths, respectively.

(A) Nm.1; (B) Nm. 2.

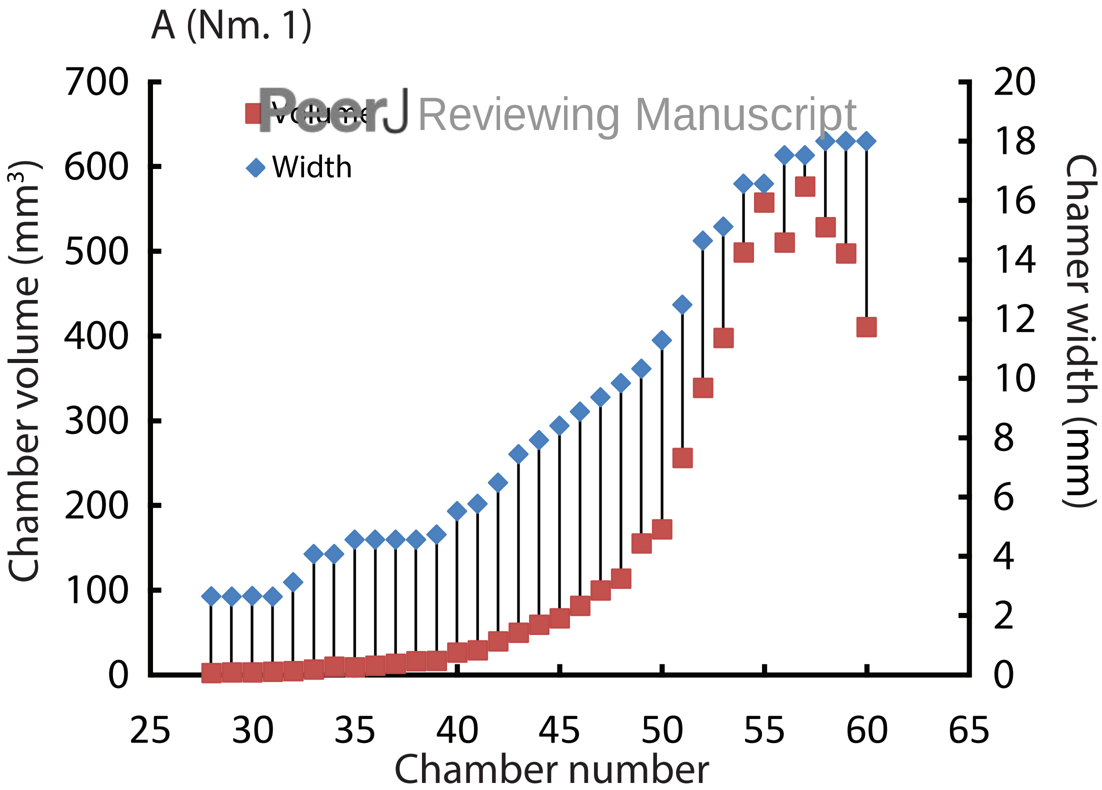
A (Nm. 1)
Volume
Width
Chamber volume (mm3)
Chamer width (mm)
Chamber number
0
100
200
300
400
500
600
700
0
2
4
6
8
10
12
14
16
18
20
25
30
35
40
45
50
55
60
65

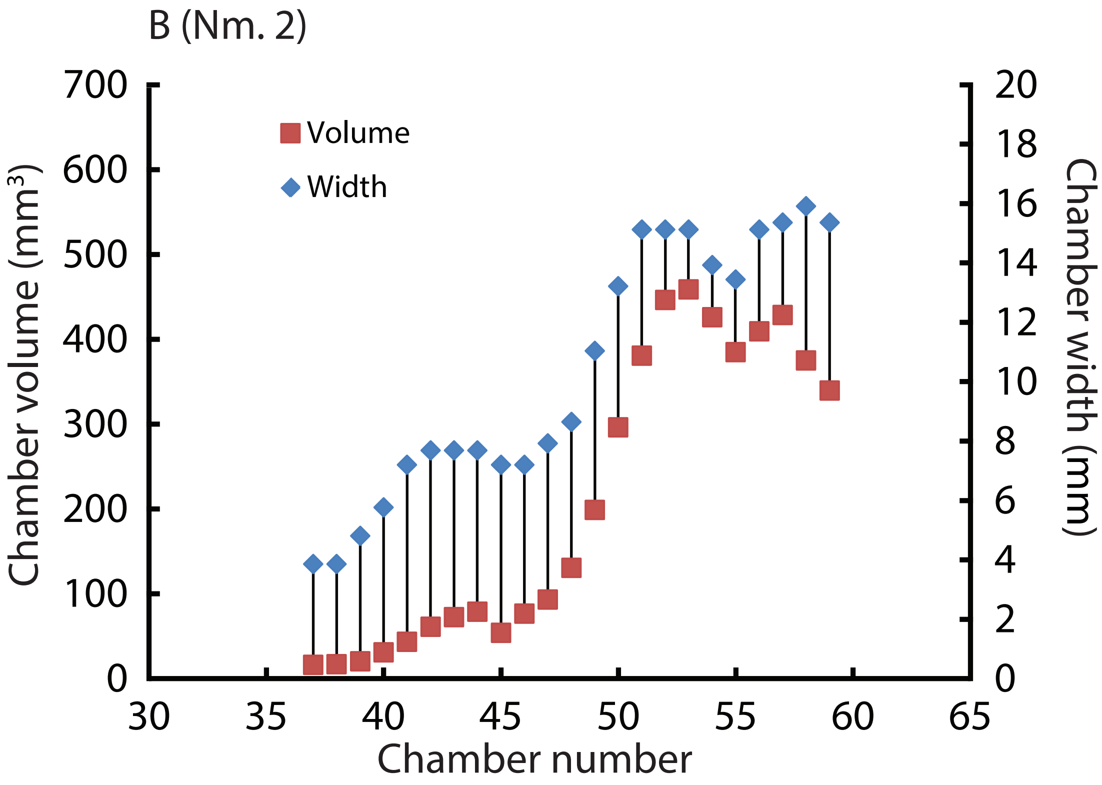
B (Nm. 2)
Volume
Width
Chamber volume (mm3)
Chamber width (mm)
Chamber number
0
100
200
300
400
500
600
700
0
2
4
6
8
10
12
14
16
18
20
30
35
40
45
50
55
60
65

Figure 7(on next page)

Volumes and widths of chambers plotted against chamber numbers in *Nautilus pompilius*. Squres and diamonds represent volumes and widths, respectively.

(A) Specimen 8; (B) Specimen 7; (C) specimen 53. Specimens with different growth trajectories were analysed.

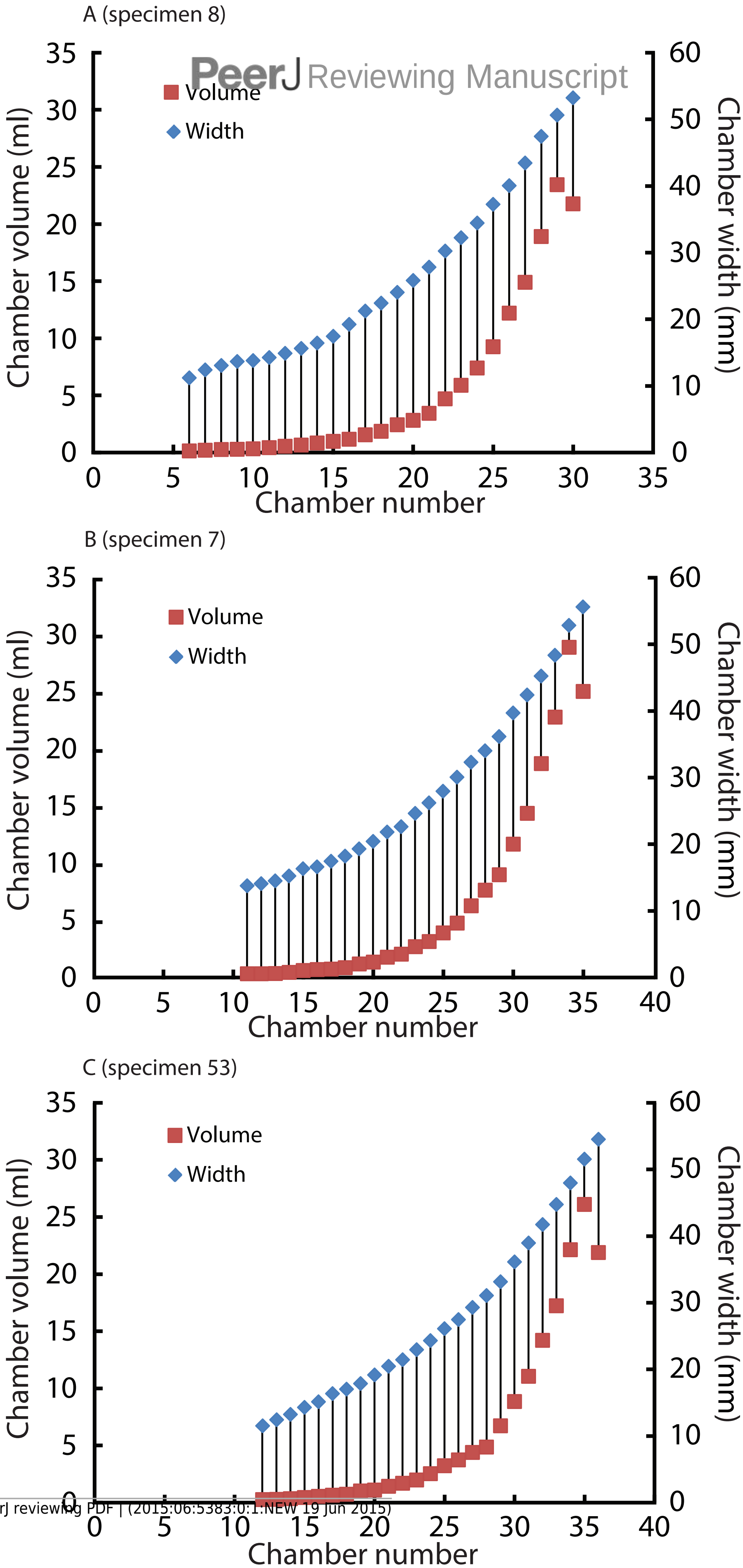
A (specimen 8)
Volume
Width
Chamber volume (ml)
Chamber width (mm)
Chamber number
B (specimen 7)
Volume
Width
Chamber volume (ml)
Chamber width (mm)
Chamber number
C (specimen 53)
Volume
Width
Chamber volume (ml)
Chamber width (mm)
Chamber number

Table 1 (on next page)

Details of the studied specimens, *Normannites mitis* from the Middle Jurassic, Switzerland, and modern *Nautilus pompilius* from the Philippines.

Specimen number	Species	Maturity	Sex	Maximum diameter (mm)	Number of chambers
Nm.1	*Normannites mitis*	Mature	Male	50	60?
Nm.2	*Normannites mitis*	Mature	Male	49	59?
7	*Nautilus pompilius*	Mature	Female	189	35
8	*Nautilus pompilius*	Mature	Female	152	30
10	*Nautilus pompilius*	Mature	Female	175	32
11	*Nautilus pompilius*	Mature	Female	165	30
12	*Nautilus pompilius*	Mature	Female	168	33
15	*Nautilus pompilius*	Mature	Female	189	33
16	*Nautilus pompilius*	Mature	Male	183	33
17	*Nautilus pompilius*	Mature	Male	183	33
20	*Nautilus pompilius*	Immature	Indet.	105	26
23	*Nautilus pompilius*	Immature	Indet.	112	26
30	*Nautilus pompilius*	Immature	Indet.	147	30
31	*Nautilus pompilius*	Immature	Indet.	136	29
32	*Nautilus pompilius*	Immature	Indet.	136	32
33	*Nautilus pompilius*	Immature	Indet.	135	27
34	*Nautilus pompilius*	Immature	Indet.	144	32
35	*Nautilus pompilius*	Immature	Indet.	124	28
36	*Nautilus pompilius*	Immature	Indet.	157	37
38	*Nautilus pompilius*	Mature	Male	150	31
39	*Nautilus pompilius*	Mature	Male	147	32
40	*Nautilus pompilius*	Mature	Male	151	30
41	*Nautilus pompilius*	Mature	Male	184	34
42	*Nautilus pompilius*	Mature	Female	169	33
43	*Nautilus pompilius*	Mature	Male	155	31
44	*Nautilus pompilius*	Mature	Male	164	35
46	*Nautilus pompilius*	Mature	Male	160	31
48	*Nautilus pompilius*	Mature	Male	165	35
51	*Nautilus pompilius*	Mature	Female	179	33
53	*Nautilus pompilius*	Mature	Male	181	36
54	*Nautilus pompilius*	Mature	Male	164	29
56	*Nautilus pompilius*	Mature	Female	176	32

Table 2 (on next page)

Raw data of measured chamber volumes and widths in *Normannites mitis*.

Normannites mitis				
Specimen	Nm. 1		Nm. 2	
Chamber	Volume (mm^3)	Width (mm)	Volume (mm^3)	Width (mm)
25	0.9	–	–	–
26	1.3	–	–	–
27	2.0	–	1.6	–
28	2.1	2.6	2.5	–
29	2.6	2.6	3.0	–
30	2.9	2.7	3.8	–
31	3.4	2.6	4.8	–
32	4.2	3.1	5.3	–
33	6.0	4.1	7.4	–
34	9.6	4.1	8.8	–
35	8.6	4.6	11.3	–
36	10.7	4.6	12.4	–
37	12.9	4.6	16.2	3.9
38	16.0	4.6	16.8	3.9
39	16.2	4.7	20.4	4.8
40	26.1	5.5	30.8	5.8
41	28.9	5.8	43.1	7.2
42	39.2	6.5	61.0	7.7
43	49.7	7.4	72.4	7.7
44	59.1	7.9	78.6	7.7
45	66.7	8.4	54.0	7.2
46	81.4	8.9	76.3	7.2
47	99.4	9.4	93.1	7.9
48	113.3	9.8	130.4	8.6
49	155.1	10.3	198.6	11.0
50	171.8	11.3	296.0	13.2
51	255.9	12.5	380.5	15.1
52	338.7	14.6	446.4	15.1
53	397.6	15.1	458.6	15.1
54	498.5	16.6	425.7	13.9
55	557.4	16.6	384.6	13.4
56	510.2	17.5	409.1	15.1
57	576.1	17.5	428.5	15.4
58	528.4	18.0	375.1	15.9
59	497.3	18.0	339.3	15.4
60	410.5	18.0	–	–

Table 3(on next page)

Raw data of measured chamber volumes in *Natutilus pompilius*.

Nautilus pompilius										
	Volumes (ml)									
Chamber	7	8	10	11	12	15	16	17	20	23
1	0.0011	0.0080	0.0082	0.0118	0.0139	0.0088	0.0099	0.0101	0.0153	0.0120
2	0.0123	0.0331	0.0257	0.0416	0.0384	0.0317	0.0145	0.0307	0.0329	0.0370
3	0.0468	0.1013	0.0760	0.1056	0.1091	0.0866	0.0424	0.0882	0.0922	0.1440
4	0.1142	0.1951	0.1539	0.1980	0.1809	0.1571	0.1109	0.1584	–	0.1904
5	0.1837	0.2417	0.2028	0.2214	0.2050	0.2032	0.1859	1.9870	0.2939	0.1658
6	0.2236	0.1264	0.1397	0.1244	0.1081	0.1327	0.2182	1.2660	0.1387	–
7	0.1287	0.1987	0.1736	0.2603	0.1742	0.1711	0.1610	0.1911	0.1504	0.1875
8	0.1767	0.2520	0.2027	0.2639	0.2046	0.1654	0.2183	0.2065	0.1695	0.2451
9	0.2265	0.2800	0.2472	0.3593	0.2370	0.2352	0.2730	0.2418	0.2092	0.3563
10	0.2619	0.3126	0.2873	0.4043	0.3378	0.2344	0.3047	0.2709	0.2314	0.3615
11	0.3097	0.4201	0.3461	0.4913	0.3364	0.2671	0.3856	0.3332	0.3010	0.2962
12	0.3254	0.5510	0.4246	0.5882	0.3992	0.3542	0.4402	0.4326	0.4017	0.5029
13	0.3419	0.6398	0.4958	0.6988	0.4677	0.4407	0.5293	0.4632	0.3846	0.6454
14	0.4342	0.8348	0.6386	0.9175	0.5496	0.5297	0.6218	0.5654	0.5069	0.7712
15	0.5986	0.9723	0.7534	1.1123	0.7096	0.5844	0.7034	0.7108	0.5902	0.8968
16	0.6954	1.1514	0.9129	1.2902	0.8697	0.6870	0.8370	0.8858	0.7431	1.0808
17	0.7329	1.5420	0.9722	1.5716	0.9987	0.8377	1.1188	1.0799	0.9711	1.3026
18	0.8595	1.8436	1.2630	2.0393	1.1376	1.0711	1.3181	1.3902	1.1740	1.5484
19	1.1690	2.4328	1.6209	2.3768	1.4889	1.4076	1.6280	1.7581	1.5174	1.7800
20	1.3495	2.8077	1.6611	3.1048	1.8336	1.6886	1.8692	2.2017	1.8071	2.4023
21	1.7666	3.4284	2.2127	3.8014	2.2195	2.2858	2.3806	2.7137	2.2284	2.8600
22	2.0429	4.7002	2.4138	5.1772	2.8784	2.6827	3.0621	2.9842	2.8115	3.4343
23	2.6836	5.8684	3.6654	6.4984	3.4312	3.0022	3.8081	4.2956	3.3740	4.4262
24	3.1432	7.3975	3.9932	6.3292	4.0784	3.9945	4.8836	5.7708	4.3020	5.5624
25	3.8981	9.2433	5.9550	10.8780	4.8802	5.2016	6.4403	6.5720	5.5132	6.8422
26	4.7613	12.1851	7.2257	13.0345	6.1415	6.9912	7.7378	8.3211	6.5154	8.3682
27	6.2645	14.8837	9.1428	15.1136	7.1537	6.9741	10.2469	9.7510	–	–
28	7.6362	18.9061	11.6261	15.0097	9.3969	9.9014	11.9939	12.6750	–	–
29	8.9947	23.4334	14.3625	18.0443	11.4332	13.0762	15.4993	15.4005	–	–
30	11.6532	21.7685	18.6543	16.2038	13.7770	15.9414	18.4287	17.8146	–	–
31	14.3670	–	22.4427	–	17.3911	21.2605	21.4919	22.5759	–	–
32	18.7249	–	25.6854	–	19.8835	25.8978	26.6814	25.5356	–	–
33	22.7825	–	–	–	19.3914	23.7399	21.6118	29.6341	–	–
34	28.9011	–	–	–	–	–	–	–	–	–
35	25.0228	–	–	–	–	–	–	–	–	–

36	–	–	–	–	–	–	–	–	–	–

Nautilus pompilius										
	Volumes (ml)									
Chamber	30	31	32	33	34	35	36	38	39	40
1	0.0009	0.0081	0.0015	0.0081	0.0076	0.0010	0.0216	0.0098	0.0106	0.0101
2	0.0093	0.0307	0.0112	0.0138	0.0238	0.0151	0.0566	0.0283	0.0415	0.0413
3	0.0491	0.1274	0.0372	0.0523	0.0673	0.0441	0.1162	0.0987	0.0610	0.1276
4	0.1152	0.0900	0.1024	–	–	0.1044	0.1356	0.1778	0.1955	0.2445
5	0.2002	0.1677	0.1703	0.2591	0.1836	0.1951	0.0903	0.2302	0.2274	0.2826
6	0.2263	0.2333	0.2108	0.3325	0.0731	0.1551	0.0677	0.1288	0.1437	0.1377
7	0.1298	0.1515	0.1059	0.1488	0.1445	0.1211	0.0875	0.1754	0.2137	0.1577
8	0.2507	0.1968	0.1578	0.2810	0.1506	0.2130	0.1325	0.2319	0.2327	0.2791
9	0.2457	0.2774	0.1513	0.3327	0.1912	0.2311	0.1384	0.2424	0.2748	0.3210
10	0.3184	0.3346	0.2389	0.3967	0.2178	0.3198	0.1650	0.3559	0.3628	0.3354
11	0.3811	0.4392	0.2743	0.4897	0.2891	0.3354	0.1998	0.3528	0.3506	0.4696
12	0.4743	0.4943	0.2953	0.5830	0.2969	0.4166	0.2167	0.4391	0.4582	0.5265
13	0.5728	0.5368	0.3519	0.6721	0.3613	0.4578	0.2776	0.5343	0.5336	0.6694
14	0.6597	0.5660	0.4364	0.7652	0.4548	0.4956	0.3469	0.6659	0.5510	0.7933
15	0.8527	0.6376	0.4978	0.9763	0.5328	0.6623	0.3984	0.8642	0.7349	0.9906
16	0.9906	0.9415	0.5625	1.1348	0.6799	0.8069	0.4671	1.0654	0.8903	1.1742
17	1.2034	1.2099	0.6816	1.5905	0.8066	0.9817	0.5594	1.2510	1.1273	1.4877
18	1.5362	1.4315	0.8131	1.7629	0.9474	1.2012	0.7268	1.5251	1.3187	1.8743
19	1.7694	1.7856	0.9522	2.2513	1.2071	1.3979	0.8601	1.8645	1.6630	2.3415
20	2.0389	1.9788	1.1264	3.0569	1.4379	1.8163	0.9568	2.3037	2.1185	2.8293
21	2.8880	2.6252	1.4726	3.5649	1.7398	2.2560	1.1435	3.0019	2.5387	3.4876
22	3.3829	3.0792	1.5172	4.5086	2.0732	2.7278	1.3670	3.8435	3.1226	4.1792
23	3.6387	4.1283	2.0698	5.8497	2.6354	3.5553	1.4716	5.0250	4.3051	5.2172
24	5.5978	4.8777	2.5775	7.8330	3.0635	4.2451	1.9052	5.9666	5.0770	6.9681
25	6.6551	6.6584	2.9776	10.0561	3.7968	5.6042	2.1254	7.4867	6.4071	9.1711
26	8.4330	8.2790	3.7357	12.3302	4.6313	7.0547	2.4165	9.5045	7.9895	11.4558
27	10.9828	10.7209	4.2277	16.8159	5.7833	8.7436	3.1417	12.3553	9.9455	14.8504
28	14.0144	13.7381	5.9748	–	6.7042	11.2815	3.9028	15.4332	12.1152	18.7030
29	17.9875	16.9861	6.9056	–	8.9703	–	4.0146	19.5149	16.8772	21.2875
30	22.9906	–	8.7325	–	10.3012	–	5.5218	22.3363	19.1758	20.7897
31	–	–	11.0929	–	13.7366	–	6.4224	21.7169	22.8448	–
32	–	–	13.4910	–	16.1578	–	8.3757	–	10.9346	–
33	–	–	–	–	–	–	9.7338	–	–	–
34	–	–	–	–	–	–	13.6863	–	–	–
35	–	–	–	–	–	–	15.1073	–	–	–

36	–	–	–	–	–	–	19.3678	–	–	–

Nautilus pompilius										
					Volumes (ml)					
Chamber	41	42	43	44	46	48	51	53	54	56
1	0.0100	0.0054	0.0090	0.0050	0.0265	0.0047	0.0175	0.0061	0.0100	0.0093
2	0.0292	0.0247	0.0306	0.0186	0.0771	0.0183	0.0470	0.0181	0.0342	0.0315
3	0.0905	0.0708	0.0881	0.0496	0.1503	0.0468	0.1091	0.0549	0.0913	0.0873
4	0.1417	0.1532	0.1587	0.1075	0.1971	0.0971	0.1735	0.1069	0.1690	0.1472
5	0.2076	0.2127	0.2030	0.1600	0.1691	0.1455	0.1890	0.1296	0.1763	0.2053
6	0.1124	0.1729	0.1402	0.1743	0.1699	0.1296	0.1049	0.0991	0.0946	0.2054
7	0.1508	0.1493	0.1831	0.1235	0.2227	0.0904	0.1476	0.0782	0.2062	0.1376
8	0.1697	0.2169	0.2357	0.1846	0.2459	0.1272	0.1975	0.1243	0.1836	0.1697
9	0.2163	0.2819	0.2991	0.1938	0.3018	0.1317	0.2505	0.1579	0.2436	0.2927
10	0.2786	0.3644	0.3365	0.2052	0.3498	0.1749	0.2403	0.1804	0.3114	0.3502
11	0.3207	0.4320	0.3932	0.2967	0.4234	0.1962	0.3590	0.2276	0.3474	0.3969
12	0.4028	0.5334	0.4842	0.3297	0.4885	0.2544	0.3641	0.2631	0.3622	0.4777
13	0.3789	0.6502	0.5946	0.4074	0.6444	0.2892	0.4552	0.2786	0.4824	0.5308
14	0.3697	0.8009	0.7316	0.4628	0.7167	0.3641	0.5052	0.3390	0.5973	0.7307
15	0.4970	1.1199	0.8541	0.5346	0.9162	0.4755	0.6910	0.4319	0.7167	0.9280
16	0.7079	1.3768	1.0209	0.6888	1.1237	0.5788	0.8284	0.5339	0.9275	1.0657
17	0.8187	1.6980	1.3506	0.8180	1.4206	0.7132	0.9799	0.6473	1.0603	1.3458
18	0.9482	2.1715	1.5373	0.9756	1.5012	0.7694	1.2509	0.7253	1.3217	1.4686
19	1.1905	2.5023	1.9608	1.2337	2.1029	0.9727	1.4561	1.0164	1.5396	1.8512
20	1.4391	3.1098	2.1780	1.5515	2.4645	1.2410	1.7334	1.0873	1.9675	2.3222
21	1.7595	4.1807	2.9540	1.9814	3.2696	1.4992	2.1757	1.4246	2.4795	2.8080
22	2.1740	5.2048	3.5435	2.6261	3.7837	1.9494	2.6698	1.6820	3.0712	3.4655
23	2.6913	6.7107	4.6642	2.7189	4.6898	2.2113	3.5267	1.9744	3.6531	4.4481
24	3.3197	8.3822	5.6355	4.1850	6.2850	2.6959	3.8889	2.5256	4.6271	5.2782
25	3.9711	9.8258	7.2365	4.8333	7.7151	3.3410	5.4467	3.2210	5.7637	6.6173
26	5.1796	14.0874	8.8481	6.3843	9.6012	4.1416	7.0138	3.7303	7.4533	8.4093
27	6.3708	16.9760	10.8568	7.8972	12.4969	5.2332	8.5615	4.3930	9.1647	10.4171
28	7.3239	20.3430	13.3318	10.4022	16.2270	6.3615	10.4667	4.8603	10.4041	13.1087
29	9.5327	25.8620	16.3558	13.1177	19.5241	7.5145	13.5815	6.7250	13.7364	15.5874
30	11.9083	24.6416	18.0790	17.3703	24.7367	9.4214	17.3426	8.8509	18.1738	20.3345
31	14.4140	–	20.2377	20.7735	20.2453	12.4135	20.6539	11.0477	22.7498	22.5689
32	18.5821	–	–	27.8035	–	15.0377	25.8738	14.1953	24.6066	19.6485
33	23.3349	–	–	27.8442	–	18.3685	21.4921	17.2212	15.7064	–
34	27.2882	–	–	–	–	22.6245	–	22.1384	–	–
35	–	–	–	–	–	26.4088	–	26.0839	–	–

36	–	–	–	–	–	–	–	21.8776	–	–

Table 4(on next page)

Raw data of measured chamber widths of *Natutilus pompilius*.

Nautilus pompilius			
	Widths (mm)		
Chambers	Specimen 8	Specimen 7	Specimen 53
6	–	–	–
7	–	–	–
8	–	–	–
9	–	–	–
10	–	–	–
11	13.8	–	13.8
12	14.1	11.5	14.1
13	14.5	12.4	14.5
14	15.2	13.2	15.2
15	16.3	14.2	16.3
16	16.6	15.1	16.6
17	17.4	16.3	17.4
18	18.2	17.0	18.2
19	19.3	17.8	19.3
20	20.4	19.1	20.4
21	21.8	20.4	21.8
22	22.6	21.4	22.6
23	24.6	22.9	24.6
24	26.2	24.3	26.2
25	30.0	26.1	30.0
26	30.1	27.4	30.1
27	32.3	29.2	32.3
28	34.0	31.0	34.0
29	36.2	33.1	36.2
30	39.7	36.1	39.7
31	42.4	38.9	42.4
32	45.2	41.7	45.2
33	48.3	44.7	48.3
34	52.8	47.9	52.8
35	55.6	51.5	55.6
36	–	54.5	–

Table 5(on next page)

Results of statistical tests (analyses of the residual sum of squares) comparing linear regressions of males and female.

N, number of samples; RSS; residual sum of squares; DF, degree of freedom; ns, not significant; s; significant.

Comparison	N (male)	N (female)	RSS (male)	RSS (female)	DF (male)	DF (female)	t	Siginificance
Chamber number vs. chamber volume (between the 1st and 5th chambers))	60	45	59.9	4601	58	43	0.005	ns (P>0.5)
Chamber number vs. chamber volume (from the 6th chamber)	332	243	108.3	104.0	330	240	16.8	s (P<0.05)
Maximum diameter vs. number of chambers	12	9	46.5	14.6	10	7	1.9	s (P<0.1)
Maximum diameter vs. total volume of phragmocone	12	9	927.6	721.0	10	7	2.2	s (P<0.1)

Table 6(on next page)

Results of a statistical test (an analysis of the residual sum of squares) comparing nonlinear regressions of males and females.

RSS; residual sum of squares; DF, degree of freedom; ns, not significant; s; significant.

Comparison	RSS (total)	RSS (male)	RSS (female)	DF (male)	DF (female)	F	Siginificance
Chamber number vs. chamber volume (from the 6th chamber)	2775.3	1670.0	1040.4	332	243	4.55	s (P<0.1)